PHYSICAL REVIEW B **74**, 220502(R) (2006)

Superconductivity in noncentrosymmetric $Mg_{10}Ir_{19}B_{16}$

T. Klimczuk,[1,2,*] Q. Xu,[3] E. Morosan,[1] J. D. Thompson,[4] H. W. Zandbergen,[1,3] and R. J. Cava[1]
[1]*Department of Chemistry, Princeton University, Princeton, New Jersey 08544, USA*
[2]*Faculty of Applied Physics and Mathematics, Gdansk University of Technology, Narutowicza 11/12, 80-952 Gdansk, Poland*
[3]*National Centre for HREM, Kavli Institute of Nanoscience, Delft University of Technology, 2628 CJ Lorentzweg 1, Delft, The Netherlands*
[4]*Condensed Matter and Thermal Physics, Los Alamos National Laboratory, Los Alamos, New Mexico 87545, USA*
(Received 25 August 2006; revised manuscript received 17 October 2006; published 5 December 2006)

$Mg_{10}Ir_{19}B_{16}$, a previously unreported compound in the Mg-Ir-B chemical system, is found to be superconducting at temperatures near 5 K. The fact that the compound exhibits a range of superconducting temperatures between 4 and 5 K suggests that a range of stoichiometries is allowed, though no structural evidence for this is observed. The compound has a large, noncentrosymmetric, body centered cubic unit cell with $a=10.568$ Å, displaying a structure type for which no previous superconductors have been reported.

DOI: 10.1103/PhysRevB.74.220502 PACS number(s): 74.10.+v, 74.70.Dd, 74.25.Ha, 74.25.Fy

INTRODUCTION

In the past five years, a variety of new superconducting materials have been discovered. Some of these materials are under continuing study because they exhibit unusual properties or structures, e.g., $Na_{0.3}CoO_2 \cdot 1.3H_2O$, which displays superconductivity in a two-dimensional CoO_2 lattice,[1] $PuMGa_5$ (M=Co,Rh), the first Pu-based superconductors,[2,3] and the pyrochlore superconductors $Cd_2Re_2O_7$,[4] MOs_2O_6 (M=K,Rb).[5,6] Also of interest have been superconducting materials based on light elements such as MgB_2,[7] $MgCNi_3$,[8] C_6Yb, and C_6Ca,[9] and the quaternary intermetallics $LnNi_2B_2C$.[10] In conventional electron-phonon coupled superconductivity, compounds based on light elements are expected to be favorable due to the correspondingly high phonon frequencies they display, suggesting a viable avenue in the search for new superconducting materials.

An important feature of almost every known superconductor is the existence of inversion symmetry in the crystal structure—a key concept for the formation of conventional Cooper pairs. The lack of superconductivity in MnSi, for example, has been attributed to its lack of inversion symmetry.[11] For this reason, the recent reports of superconductivity in noncentrosymmetric $CePt_3Si$,[12] Li_2Pd_3B,[13] and Li_2Pt_3B (Ref. 14) have stimulated significant efforts to understand and predict unconventional behavior in these compounds.[15–18]

Here we report the discovery of a light element based ternary intermetallic superconductor $Mg_{10}Ir_{19}B_{16}$. The compound, synthesized by conventional methods, is superconducting at a critical temperature of about 5 K. A small range of superconducting transition temperatures is observed, indicating that the compound occurs over a range of compositions. This material has a body centered cubic crystal structure with a large unit cell, $a=10.568$ Å, and, consequently, a complex formula. The space group of the compound, I-43m, indicates that $Mg_{10}Ir_{19}B_{16}$ is one of the rare examples of a noncentrosymmetric superconducting material. There are no previously known superconductors, or intermetallic compounds, with an analogous crystal structure. This paper reports the synthesis and basic superconducting properties of the phase. The details of the crystal structure determination, which has been performed by quantitative electron diffraction and imaging methods, will be described elsewhere.[19]

EXPERIMENTAL

During an investigation of the Mg-Ir-B chemical system, superconductivity was observed to occur in a region of the phase diagram near the molar ratio 1:2:2. An extensive series of 0.2 g polycrystalline samples was made to determine the composition of the superconducting phase. Materials were synthesized by standard solid state reaction of pure elements: bright Mg flakes (99% Aldrich Chemical), fine Ir powder (99.9% Alfa Aesar), and amorphous B powder (99.5%, Cerac). After initial mixing, the starting materials were pressed into pellets, wrapped in Ta foil, placed in an Al_2O_3 boat, and fired in a quartz-tube furnace under a 95% Ar/5% H_2 atmosphere. The first furnace treatment was for 30 min at 600 °C, followed by 1 h at 900 °C. After cooling, the samples were reground with an additional 20% of Mg, pressed into pellets, and placed back in the furnace for 1 h at 900 °C. The sample purity was checked by powder x-ray diffraction using Cu $K\alpha$ radiation on a diffractometer equipped with a diffracted beam monochrometer. The unit cell parameter was refined from the x-ray data using the profile refinement program TOPAS version 2.1 (Bruker AXS). Zero field cooling dc ($H_{dc}=20$ Oe) and ac ($H_{dc}=5$ Oe, $H_{ac}=3$ Oe, $f=10$ kHz) magnetizations were measured in the range of 2–6 K (PPMS-Quantum Design). The field dependence of the magnetization was measured at 2 K. Resistivity measurements were made using a standard ac four-probe technique on polycrystalline pellets cut into dimensions of approximately $2.2\times0.9\times0.9$ mm.

RESULTS

The isolation of the superconducting phase was accomplished by the standard method of comparing the strength of the observed superconducting diamagnetic signal with characteristic features of the powder diffraction patterns from the samples. This process was substantially simplified by the fact

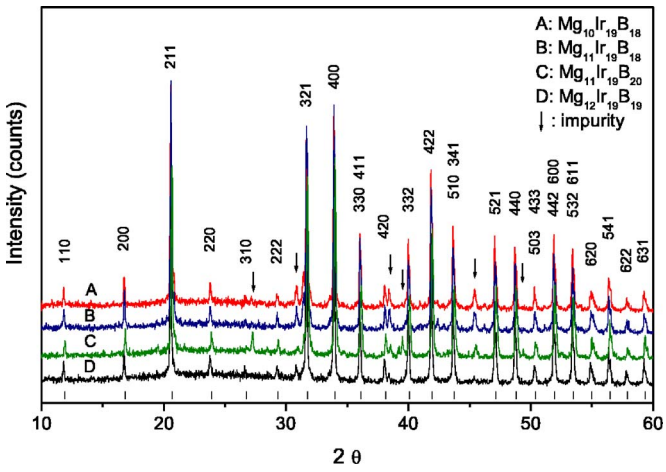

FIG. 1. (Color online) Powder x-ray diffraction patterns (Cu $K\alpha$ radiation) for compounds of nominal composition: $Mg_{10}Ir_{19}B_{18}$ (a), $Mg_{11}Ir_{19}B_{18}$ (b), $Mg_{11}Ir_{19}B_{20}$ (c), and $Mg_{12}Ir_{19}B_{19}$ (d). The latter composition is the most nearly phase pure. Vertical bars at the bottom represent the Bragg peak positions for a body centered cubic cell with refined cell parameter $a=10.5678$ Å. Miller indices for each peak are shown, and impurity phase peak positions are marked with arrows.

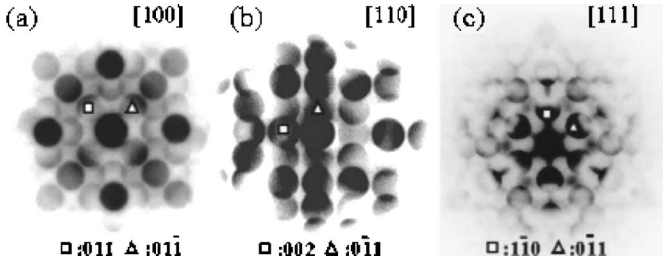

FIG. 2. Convergent beam electron diffraction patterns for $Mg_{10}Ir_{19}B_{16}$ along (a) [100], (b) [110], (c) [111] show clearly 4 mm, *m*, 3 m symmetry, respectively. This indicates that the space group of the material is *I*-43*m*.

that there are no superconducting compounds in the binary Mg, Ir, B systems with transition temperatures near the 5 K observed for the new superconducting material, and the fact that the new superconducting compound gives an excellent, characteristic powder diffraction pattern. The initial round of syntheses showed that the largest superconducting signals were seen for nominal Mg:Ir:B compositions near 1:2:2 that showed a powder diffraction pattern straightforwardly indexed on a body centered cubic unit cell of dimension approximately 10.57 Å. Samples in finer composition intervals were then synthesized in order to refine the composition of the superconductor. The x-ray diffraction patterns of four Mg-Ir-B samples in the vicinity of the optimal composition are presented in Fig. 1. The patterns are dominated by a very well crystallized, high symmetry compound, and are all very nearly single phase. The vertical bars at the bottom of Fig. 1 show the Bragg peak positions for a body centered cubic structure. The refined crystallographic cell parameter from 22 reflections is $a=10.56782(4)$ Å. No compound with this lattice type and unit cell dimension has been previously reported in the Mg-Ir-B chemical system, or any related chemical systems.[20] By using the *I*-43*m* space group and the unit cell $a=10.56782(4)$ Å, virtually all the peaks in the XRD patterns near the optimal superconducting composition can be indexed. Figure 1 shows that the sample with the nominal composition $Mg_{12}Ir_{19}B_{19}$ is very nearly single phase, with less than 5% detectable impurity phase by XRD. The large superconducting signal seen for this sample along with its near phase purity indicates that this is the new superconducting compound.

Due to the very large crystallographic unit cell, complex formulas are possible for this compound, and the exact composition of the phase can only be determined by detailed structural analysis. To determine the space group we employed convergent beam electron diffraction (CBED) methods (Fig. 2). The symmetries along the [100] and [111] directions are 4 mm and 3 m, respectively. The CBED pattern along [110] [Fig. 2(c)] unambiguously shows that the symmetry along this direction is *m*, not 2 mm, requiring that the body centered space group of the new phase is noncentrosymmetric *I*-43*m* (No. 217) rather than centrosymmetric *Im*-3*m*.[21] Next, using quantitative analysis of electron diffraction, the composition ($Mg_{10}Ir_{19}B_{16}$) and atom positions were determined. These are presented in Table I. The details of the structure refinement are reported elsewhere.[19] This formula is very close to the optimal nominal composition of $Mg_{12}Ir_{19}B_{19}$. The higher amount of Mg required to make the highest purity sample is a result of volatilization of Mg during the synthesis, and is analogous to what was observed in the synthesis of $MgCNi_3$.[8] Similarly, between 15 and 20 % excess B is needed to make the purest phase, significantly less than the amount of excess C needed to make optimal

TABLE I. Crystallographic data for $Mg_{10}Ir_{19}B_{16}$ from quantitative electron diffraction analysis (Ref. 19). Space group *I*-43*m* (No. 217), $a_0=10.568$ Å.

Atom (site)	x	y	z	B (Å^2)	Occupancy
Ir1 (2a)	0	0	0	3.04(3)	1
Ir2 (12d)	0	0.25	0.5	0.99(1)	1
Ir3 (24g)	0.07025(5)	0.25248(4)	0.25248	1.19(1)	1
Mg1 (8c)	0.3331(2)	0.3331	0.3331	0.15(2)	1
Mg2 (12e)	0	0	0.3473(3)	0.15(2)	1
B1 (8c)	0.1127(3)	0.1127	0.1127	0.08(9)	1
B2 (24g)	0.1639(2)	0.1639	0.4140(3)	0.48(6)	1

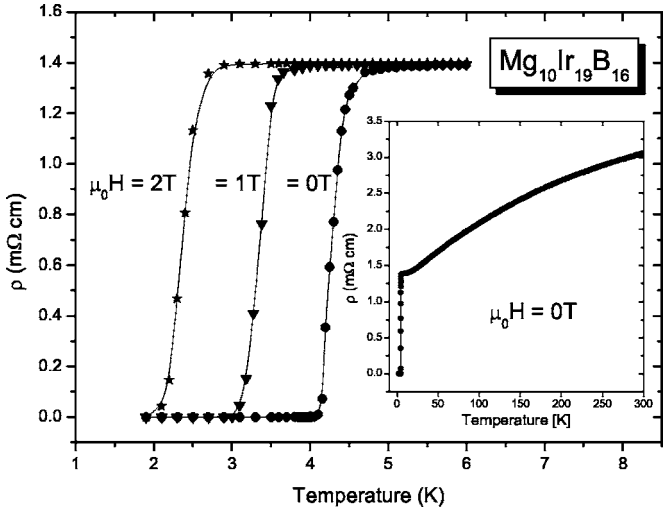

FIG. 3. Magnetic-field dependence of the electrical resistivity for $Mg_{10}Ir_{19}B_{16}$ (nominal composition $Mg_{12}Ir_{19}B_{19}$)—detail near the superconducting transition. The inset shows the temperature dependent resistivity between 2 K and 300 K

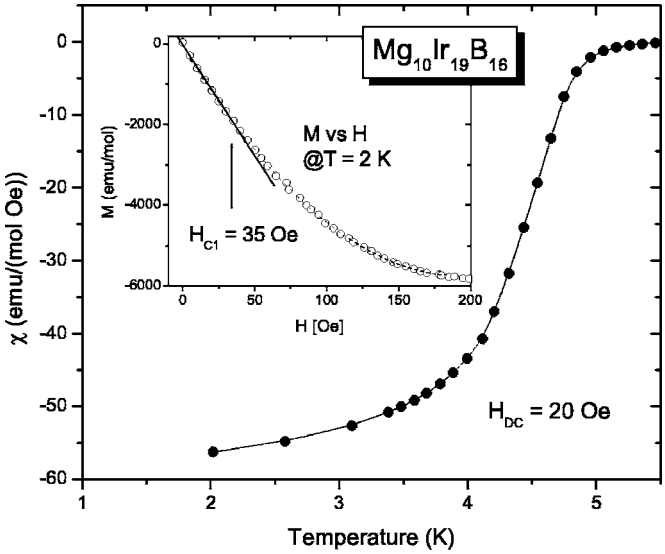

FIG. 4. dc magnetization characterization of the superconducting transition in $Mg_{10}Ir_{19}B_{16}$ (nominal composition $Mg_{12}Ir_{19}B_{19}$). The inset shows magnetization vs applied magnetic field dependence at 2 K.

$MgCNi_3$ by the same synthetic method. The excess B occurs in elemental form in the sample, and was observed in the HREM investigation.

Figure 3 presents the temperature and magnetic-field dependence of the electrical resistivity of $Mg_{10}Ir_{19}B_{16}$. The main panel shows the temperature range near the superconducting transition. Under zero applied magnetic field, the midpoint of the resistive transition is at 4.4 K, and the 10–90 % transition width is 0.4 K. When an external magnetic field is applied, the critical temperature decreases to 3.35 K and 2.4 K at 1 T and 2 T, respectively. More measurements under higher magnetic field and at lower temperature would be necessary to make a good estimate of $H_{C2}(0)$, but our results suggest, using the Werthamer-Helfand-Hohenberg (WHH) formula $H_{C2}(0) \cong -0.7T_C(dH_{C2}/dT)|_{T_C}$,[22] that $H_{C2}(0)$ is low, not exceeding 3 T. The inset of Fig. 3 presents the temperature dependent resistivity between 2 K and 300 K. The normal-state resistivity is rather high, about 3 mΩ cm at $T=300$ K, about 35 times higher than what is observed for polycrystalline $MgCNi_3$.[8] This suggests that the excess boron present is located at the grain boundaries of the polycrystalline sample, and that the measured value of the resistivity is not intrinsic. Measurements on single crystals are needed to determine detailed information about the transport properties of the new superconductor.

To characterize the superconducting transition of $Mg_{10}Ir_{19}B_{16}$, zero-field cooling dc magnetization was measured between the temperatures 2 K–6 K (Fig. 4), in an applied field of 20 Oe. The shielding volume fraction from this measurement is estimated to be near 100%. The field dependent magnetization curve, $M(H)$, at 2 K is shown in the inset of Fig. 4. Magnetization loops (not shown here) were made at the same temperature, indicating a substantial critical current density, a strong indication for bulk superconductivity. H_{C1} at 2 K, estimated as the field where the lowest field data deviate from a straight line, is approximately 35 Oe. This low H_{C1} accounts for much of the rounding seen in the measurement of the transition in the applied field of 20 Oe shown in the main panel. With an H_{C1} and H_{C2} of approximately 35 Oe and 30 000 Oe, at 2 K, respectively, $Mg_{10}Ir_{19}B_{16}$ is a type 2 superconductor with an estimated $\kappa \approx H_{C2}(2K)/H_{C1}(2K)$, of 800.

In order to measure the transition temperature more precisely, and its variation with composition, zero field ac susceptibility measurements were performed ($H_{dc}=5$ Oe, $H_{ac}=3$ Oe, $f=10$ kHz). Figure 5 shows the real part of the magnetization, M'_{ac}, for the four samples, with nominal compositions $Mg_{10}Ir_{19}B_{18}$, $Mg_{11}Ir_{19}B_{18}$, $Mg_{11}Ir_{19}B_{20}$, and $Mg_{12}Ir_{19}B_{19}$, whose powder x-ray patterns are shown in Fig. 1. The data in Fig. 5 show that the highest T_C is observed for

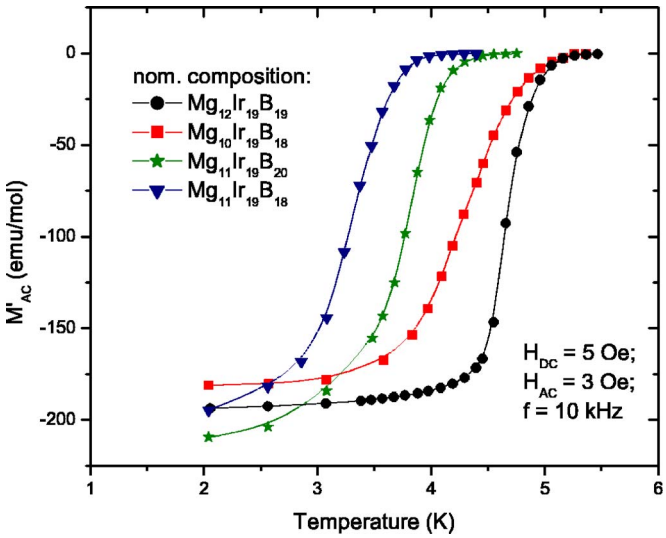

FIG. 5. (Color online) ac magnetization characterization of the superconducting transition for samples with nominal compositions $Mg_{10}Ir_{19}B_{18}$, $Mg_{11}Ir_{19}B_{18}$, $Mg_{11}Ir_{19}B_{20}$ and $Mg_{12}Ir_{19}B_{19}$.

the sample of nominal composition $Mg_{12}Ir_{19}B_{19}$—the most chemically pure sample according to the XRD measurements. Almost the same T_{Conset}, 5 K, is observed for the sample of nominal composition $Mg_{10}Ir_{19}B_{18}$, however the transition is not as sharp as is seen for all other samples, suggesting that the material is chemically inhomogeneous. For $Mg_{11}Ir_{19}B_{20}$ and $Mg_{11}Ir_{19}B_{18}$ the observed diamagnetism is similar, and the transitions are again relatively sharp, but T_C is lower than that observed for the optimal composition: to 4.4 K and 4 K for $Mg_{11}Ir_{19}B_{20}$ and $Mg_{11}Ir_{19}B_{18}$, respectively. The nature of the chemical variability of the superconducting phase is not currently understood; however, the fact that very little variation in lattice parameter (less than 0.05%) is observed suggests both that the chemical variability is small and that it likely involves the boron, which is much smaller than the metallic constituents Mg and Ir, and is expected to change the unit cell size only slightly if variable.

CONCLUSION

By exploring the Mg-Ir-B phase diagram in a search for light-element based intermetallic superconductors, a new ternary superconducting compound was discovered. The new intermetallic compound, $Mg_{10}Ir_{19}B_{16}$, has a noncentrosymmetric crystal structure with a large, body centered unit cell of $a=10.568$ Å. The synthesis of this compound is similar to that used in the case of $MgCNi_3$ and requires an excess of both Mg and B in the starting material. The critical temperature, T_C about 5 K, was determined by both electrical resistivity and magnetization measurements. $Mg_{10}Ir_{19}B_{16}$ is a rare example of noncentrosymmetric superconducting material, and has a new intermetallic structure type. The characterization of related materials with the same structure type would be of significant interest, as would more detailed measurements of the superconducting properties to determine whether any manifestation of the noncentrosymmetric crystal structure can be observed.

ACKNOWLEDGMENTS

This work was supported by the U.S. Department of Energy, Grant No. DE-FG02-98-ER45706. The work at Delft was supported by The Nederlandse Stichting voor Fundamenteel Onderzoek der Materie (FOM). T.K. would like to thank The Foundation for Polish Science for support. The work at Los Alamos was performed under the auspices of the U.S. Department of Energy, Office of Science.

*Present address: Condensed Matter and Thermal Physics, Los Alamos National Laboratory, Los Alamos, New Mexico 87545, USA.

[1] K. Takada, H. Sakurai, E. Takayama-Muromachi, F. Izumi, R. A. Dilanian, and T. Sasaki, Nature (London) **422**, 53 (2003).

[2] J. L. Sarrao, L. A. Morales, J. D. Thompson, B. L. Scott, G. R. Stewart, F. Wastin, J. Rebizant, P. Boulet, E. Colineau, and G. H. Lander, Nature (London) **420**, 297 (2002).

[3] F. Wastin, P. Boulet, J. Rebizant, E. Colineau, and G. H. Lander, J. Phys.: Condens. Matter **15**, S2279 (2003).

[4] M. Hanawa, Y. Muraoka, T. Tayama, T. Sakakibara, J. Yamaura, and Z. Hiroi, Phys. Rev. Lett. **87**, 187001 (2001).

[5] S. Yonezawa, Y. Muraoka, Y. Matsushita, and Z. Hiroi, J. Phys.: Condens. Matter **16**, L9 (2004).

[6] S. Yonezawa, Y. Muraoka, Y. Matsushita, and Z. Hiroi, J. Phys. Soc. Jpn. **73**, 819 (2004).

[7] J. Nagamatsu, N. Nakagawa, T. Muranaka, Y. Zenitani, and J. Akimitsu, Nature (London) **410**, 63 (2001).

[8] T. He, Q. Huang, A. P. Ramirez, Y. Wang, K. A. Regan, N. Rogado, M. A. Hayward, M. K. Haas, J. J. Slusky, K. Inumara, H. W. Zandbergen, N. P. Ong, and R. J. Cava, Nature (London) **411**, 54 (2001).

[9] T. E. Weller, M. Ellerby, S. S. Saxena, R. P. Smith, and N. T. Skipper, Nat. Phys. **1**, 39 (2005).

[10] R. J. Cava, H. Takagi, H. W. Zandbergen, J. J. Krajewski, W. F. Peck, T. Siegrist, B. Batlogg, R. B. van Dover, R. J. Felder, K. Mizuhashi, J. O. Lee, H. Eisaki, and S. Uchida, Nature (London) **367**, 252 (1994).

[11] C. Pfleiderer, G. J. McMullan, S. R. Julian, and G. G. Lonzarich, Phys. Rev. B **55**, 8330 (1997).

[12] E. Bauer, G. Hilscher, H. Michor, Ch. Paul, E. W. Scheidt, A. Gribanov, Yu. Seropegin, H. Noel, M. Sigrist, and P. Rogl, Phys. Rev. Lett. **92**, 027003 (2004).

[13] K. Togano, P. Badica, Y. Nakamori, S. Orimo, H. Takeya, and K. Hirata, Phys. Rev. Lett. **93**, 247004 (2004).

[14] P. Badica, T. Kondo, and K. Togano, J. Phys. Soc. Jpn. **74**, 1014 (2005).

[15] K. V. Samokhin, E. S. Zijlstra, and S. K. Bose, Phys. Rev. B **69**, 094514 (2004).

[16] P. A. Frigeri, D. F. Agterberg, A. Koga, and M. Sigrist, Phys. Rev. Lett. **92**, 097001 (2004).

[17] K. V. Samokhin, Phys. Rev. Lett. **94**, 027004 (2005).

[18] H. Q. Yuan, D. F. Agterberg, N. Hayashi, P. Badica, D. Vandervelde, K. Togano, M. Sigrist, and M. B. Salamon, Phys. Rev. Lett. **97**, 017006 (2006).

[19] Q. Xu, T. Klimczuk, T. Gortenmulder, J. Jansen, M. A. McGuire, R. J. Cava, and H. W. Zandbergen (unpublished).

[20] Inorganic Crystal Structure Database (ICSD), Fachinformationszentrum Karlsruhe, Germany and National Institute of Standards and Technology, Gaithersburg, MD, Version 2006–1.

[21] M. Tanaka, Acta Crystallogr., Sect. A: Found. Crystallogr. **A50**, 261 (1994).

[22] N. R. Werthamer, E. Helfand, and P. C. Hohenberg, Phys. Rev. **147**, 295 (1966).